SRTM/ASTER boundary analysis

Jim Regetz, NCEAS

Last update: 13 Jul 2011

.

Brief summary of findings

- SRTM vs ASTER differences
  - ASTER is systematically lower, by 12 meters in the median case
  - … but with variability: standard deviation of $\text{ASTER}_i - \text{SRTM}_i$ is 10.1
  - ASTER also has numerous spurious spikes
  - ASTER has more high-frequency variability ("texture"), affecting slope/aspect?
- Fusion via northward exponential rampdown of boundary delta
  - eliminates elevation cliff at 60°N
  - leaves abrupt transition in SRTM/ASTER textural differences
  - introduces north-south ridging artifacts
  - (*no further treatment in this document*)
- Fusion via multiresolution spline
  - eliminates elevation cliff at 60°N
  - leaves abrupt transition in derived slope and aspect
  - unclear whether derived values of aspect and flow direction in the transition zone are acceptable
- Fusion via Gaussian weighted average of SRTM/ASTER
  - eliminates elevation cliff at 60°N
  - also smooths transition slope and aspect
  - unclear whether derived values of aspect and flow direction in the transition zone are acceptable
- Canada DEM itself has problems
  - 60°N coincides with provincial boundaries; there are clear 60°N artifacts in this layer!
  - other evident tiling artifacts too
- Other comments
  - N/S bias to aspect, flow direction computed on unprojected data at higher latitudes?

To do (possibly)

- add constant offset of 12m to ASTER
- apply low pass filter to ASTER to reduce high frequency variation?
- apply algorithm to remove spikes (… but maybe beyond scope?)

Terrain layer production methodology

For the purposes of assessing artifacts associated with the northern boundary between SRTM and ASTER, I focused on a narrow band along the 60°N boundary in Canada (Figure 1). The latitudinal extent of this band is 59.875°N- 60.125°N (i.e., 300 3" pixels straddling 60°N), and the longitudinal extent is 136°W to 96°W (i.e., 48,000 pixels wide). See Listing 1 for code. Within this focal region, I generated latitudinal profiles of mean elevation, slope, aspect, and flow direction, using the separate SRTM and ASTER component DEMs themselves, using several different fused ASTER/SRTM DEMs (see below), and using the Canadian Digital Elevation Data (CDED) as an independent reference layer (`http://www.geobase.ca/geobase/en/data/cded/index.html`). I also then computed latitudinal correlations and RMSEs between the fused layers and each of SRTM, ASTER, and CDED.

Elevation This document includes latitudinal characterizations of terrain values based on three different variants of a fused 3" ASTER/SRTM DEM. I also explored (and briefly describe below) two additional approaches to fusing the layers, but do not include further assessment of these here.

Simple fusion Naive concatenation of SRTM below 60°N with ASTER above 60°N, without applying any modifications to deal with boundary artifacts (Figure 2a).

Multiresolution spline Application of Burt & Adelson's (1983) method for blending overlapping images using multiresolution splines, as implemented in the *Enblend* software package (version 4.0, `http://enblend.sourceforge.net`). Data preparation and post-processing were handled in R (see Listing 4). As presented here, the SRTM and ASTER inputs were prepared such that the overlap zone is 75 latitudinal rows (6.75km) (Figure 2b).

Gaussian weighted average Blend of the two layers using weighted averaging such that the relative contribution of the SRTM elevation is zero at 60°N, and increases as a function of distance moving south away from 60°N (Equation 1).

$$fused_{x,y} = \begin{cases} ASTER_{x,y} & \text{above } 60°\text{N} \\ w_{x,y}ASTER_{x,y} + (1 - w_{x,y})SRTM_{x,y} & \text{below } 60°\text{N} \end{cases} \tag{1}$$

where $w_{x,y} = e^{-rD_y^2}$ and D_y is the distance from 60°N in units of pixels.

For the assessment presented here, the weighting function function was parameterized using r=0.001, producing equal weights for SRTM and ASTER at a distance of ∼2.3km (26 cells) south of the the boundary, and a relative weight for ASTER of only 1% by ∼6.1km (68 cells) (Figure 2c). See `OPTION 3` in Listing 2.

Others not shown I also experimented with some additional fusion approaches, but have excluded them from further analysis in this document.

Fused with exponential ramp north of 60°N. The first step was to take the pixel-wise difference between SRTM and ASTER in the row immediately below 60°N (i.e., the northernmost extent of SRTM). An exponentially declining fraction of this difference was then then added back into the ASTER values north of 60°N. This does a fine job of eliminating the artificial shelf and thus the appearance of a seam right along the 60°N boundary, but it does not address the abrupt transition in texture (i.e., the sudden appearance of high frequency variability moving north across the boundary). Additionally, it introduces vertical "ridges" running north from the boundary. These arise because the calculated ramps are independent from one longitudinal "column" to the next, and thus any changes in the boundary difference from one pixel to the next lead to adjacent ramps with different inclines.

Simple LOESS predictive model. This involved first calculating the difference between SRTM and ASTER everywhere south of 60°N, and then fitting a LOESS curve to these differences using the actual ASTER elevation as a predictor. I then used the fitted model to predict the ASTER-SRTM difference for each ASTER cell north of 60°N, and added a declining fraction (based on a Gaussian curve) of this difference to the corresponding ASTER elevation. Conceptually, this amounts to applying an ASTER-predicted SRTM correction to the ASTER elevation values, where the correction term has a weight that declines to zero with increasing distance (north) away from the boundary. However, this method alone didn't yield particularly promising results in removing the 60°N seam itself, presumably because adding a predicted correction at the boundary does not close the SRTM-ASTER gap nearly as efficiently as do corrections based directly on the observed SRTM vs ASTER elevation differences. I therefore haven't pursued this any further, although it (or something like it) may prove useful in combination with one of the other methods.

Slope For each of the three main fused DEM variants described above, slope was calculated using `gdaldem` (GDAL 1.8.0, released 2011/01/12):

```
$ gdaldem slope -s 111120 <input_elevation> <output_slope>
```

Note that the scale option used here is as recommended in the `gdaldem` documentation:

> "*If the horizontal unit of the source DEM is degrees (e.g Lat/Long WGS84 projection), you can use scale=111120 if the vertical' units are meters*"

The output slope raster is in units of degrees.

Aspect As was the case with slope, aspect was calculated using `gdaldem`:

```
$ gdaldem aspect -s 111120 <input_elevation> <output_aspect>
```

The output aspect raster values indicate angular direction in units of degrees, with 0=North and proceeding clockwise.

Flow direction Flow direction was calculated using the GRASS (GRASS GIS 6.4.1) `r.terraflow` module; see code listing 5. Because of a ∼30k (2^{15}) limit to the input raster dimension size in the pre-built GRASS `r.terraflow` module I used, this analysis was restricted to a smaller longitudinal subset of the data, spanning 125°W to 100°W.

The default flow direction output of this module is encoded so as to indicate *all* downslope neighbors, also known as the Multiple Flow Direction (MFD) model. However, to simplify post-processing and summarization, the results here are based on an alternative Single Flow Direction (SFD, *a.k.a.* D8) model, which indicates the neighbor associated with the steepest downslope gradient. Note that this is equivalent to what ArcGIS GRID `flowaccumulation` command does. I then recoded the output raster to use the same azimuth directions used by `gdaldem aspect`, as described above for aspect.

Latitudinal mean terrain profiles

Elevation SRTM, ASTER, and CDED all share a very similarly shaped mean elevation profile, but with differing heights (Figure 3). SRTM tends to be highest, ASTER is lowest, and CDED is intermediate. The magnitude of average difference between SRTM and ASTER is fairly consistent not only across latitudes, but also across elevations (Figure 7). The overall median difference between ASTER and SRTM (i.e., considering $\text{ASTER}_i - \text{SRTM}_i$ for all pixels i where the two DEMs co-occur) is -12 meters, with a mean of -11.65 meters, and this more or less holds (within a few meters) across the observed range of elevations (Figure 7a). However, while this average offset is broadly consistent across latitudes and across elevation zones, additional variation is evident at the pixel level. Again focusing on the pixel-wise differences, they appear to be symmetrically distributed about the mean with a standard deviation of 10.1 and quartiles ranging from -17 to -7 meters; ASTER elevations are actually greater than SRTM for 6% of pixels (see Figure 7b). Thus, although adding a constant offset of 12 meters to the ASTER DEM would clearly center it with respect to the SRTM (at least in the Canada focal region), appreciable differences would remain. Figure 7b also highlights the existence of several obviously spurious ASTER spikes of >1000m; although not shown here, these tend to occur in small clumps of pixels, perhaps corresponding to false elevation readings associated with clouds?

Not surprisingly, simple fusion produces an artificial ∼12m cliff in the mean elevation profile (Figure 3). At least in terms of mean elevation, this artifact is completely removed by both the multiresolution spline and Gaussian weighted average methods. The transition is, to the eye, slightly smoother in the former case, although ultimately this would depend on the chosen zone of overlap and on the exact parameterization of the weighting function.

Slope The mean ASTER slope is uniformly steeper than the mean SRTM slope at all latitudes in the area of overlap, by nearly 1 degree (Figure 4). However, the shape of the profile itself is nearly identical between the two. Although this may partly reflect inherent SRTM vs ASTER differences, my guess is that CGIAR post-processing of the particular SRTM product we're using has removed some of the high frequency "noise" that remains in ASTER? **[todo: check!]**

Note that the CDED tends to be flatter than both SRTM and ASTER (presumably because it is at least partially derived from contour-based data **[todo: check!]**). Moreover, this figure makes it clear that CDED has some major artifacts at regular intervals. The spike especially at 60°N (which coincides with provincial boundaries across the entirety of western Canada) means we probably need to scuttle our plans to use this DEM as a formal reference dataset for boundary analysis.

The simple fused layer exhibits a dramatic spike in slope at the immediate 60°N boundary, undoubtedly associated with the artificial elevation cliff. This artifact is eliminated by both the multiresolution spline and Gaussian weighting. However, the former exhibits a sudden step change in slope in the SRTM-ASTER overlap region, whereas the transition is smoothed out in the latter. This likely reflects the fact that the multiresolution spline effectively uses a very narrow transition zone for stitching together high frequency components of the input images, and it seems likely that these are precisely the features responsible for the shift in mean slope.

Aspect For the purposes of latitudinal profiles, aspect values were summarized using a circular mean (Equation 2).

$$\bar{x} = \text{atan2}\left(\sum_{i=1}^{n}\frac{\sin(x_i)}{n}, \sum_{i=1}^{n}\frac{\cos(x_i)}{n}\right) \tag{2}$$

where x_i is the aspect value (in radians) of pixel i.

As indicated in Figure 5, the circular mean aspect values of SRTM and ASTER are generally similar across all latitudes in the area of overlap, and mean aspect values calculated on CDED are similar at most but not all latitudes. The mean values at nearly all latitudes are directed either nearly north or nearly south, though almost always with a slight eastward rather than westward inclination. In fact, there appears to be a general bias towards aspect values orienting along the north-south axis, as is especially apparent in the rose diagrams of Figure 8. I suspect this is an artifact of our use of unprojected data, especially at these high latitudes. Because the unprojected raster is effectively 'stretched' east and west relative to the actual topography, elevational gradients along the east-west axis are artificially flattened, and the direction of dominant gradient is more likely to be along the north-south axis.

Upon further reflection, it's not clear whether these patterns of mean aspect are particular useful diagnostics, as they seems to be sensitive to subtle variations in the data. Referring again to Figure 8, note how the mean direction flips from nearly north to nearly south between the two latitudes, even though the distributions of pixel-wise aspect values are nearly indistinguishable by eye.

In any case, not surprisingly, the simple fused layer matches the SRTM aspect values south of 60°N and the ASTER aspect values north of 60°N; at the immediate boundary, the mean aspect is northward, as one would expect in the presence of a cliff artifact at the seam.

Interestingly, the aspect layers derived from the two blended DEMs (multiresolution spline and Gaussian weighted average) exhibit a consistent mean northward inclination at all latitudes in their respective fusion zones. This pattern is visually obvious at latitudes between 59.95°N and 60°N in the bottom two panels of Figure 5. This is almost certainly a signal of the blending of the lower elevation ASTER to the north with higher elevation SRTM to the south, introducing a north-facing tilt (however slight) to the data throughout this zone.

Flow direction With the exception of edge effects at the margins of the input rasters, mean ASTER-derived flow is nearly northward at all latitudes, and SRTM-derived flow is nearly northward at all but a few latitudes (Figure 6). This seems reasonable considering that most pixels in this Canada test region fall in the Arctic drainage. For unknown reasons, CDED produces southward mean flow direction at numerous latitudes, and generally seems to have a slightly more eastward tendency. As was the case with aspect, note that a general north-south bias is evident (Figure 9), again likely due to use of an unprojected raster at high latitudes.

The various fused layer profiles look as one would expect (Figure 6), although the overall lack of latitudinal variability in mean flow direction in SRTM, ASTER, and all three derived layers makes it hard to say much more than that.

Informal correlation analysis

Elevation Pearson correlations between SRTM and ASTER are quite high, typically >0.999, and RMSEs are on the order of 10-15 meters (Figures 10a and 10b). Spikes (downward for correlation, upward for RMSE) occur at some latitudes, quite possibly associated with the observed extreme spikes in the ASTER DEM itself. As expected, the multiresolution spline and Gaussian weighted average both produce layers that gradually become less similar to ASTER and more similar to SRTM moving south from 60°N, but in slightly different ways. This gradual transition is less evident when considering associations with CDED (bottom panels of Figures 10a and 10b), which in general is less correlated with SRTM, and even less with ASTER, than those two layers are with each other.

Slope The patterns of slope layer similarity are much like those described above for elevation, although the correlations are somewhat lower ($\sim$0.94 between SRTM and ASTER (Figure 11a)). RMSEs between SRTM and ASTER are approximately 2 at all latitudes where the data co-occur (Figure 11b). Another difference, echoing a pattern previously noted in the profiles of mean slope itself, is that Gaussian weighted averaging produces a layer that exhibits a gradual transition from ASTER to SRTM, whereas the multiresolution spline yields an abrupt transition. Not surprisingly, the simple fused layer is even worse, producing not only a sudden transition but also aberrant values at the fusion seam itself; note downward (upward) spikes in correlation (RMSE) at 60°N in the first column of plots in Figures 11a and 11b.

Aspect Because aspect values are on a circular scale, I calculated modified versions of the Pearson correlation coefficient using the **circular** R package function `cor.circular`. I believe this implements the formula described by Jammalamadaka & Sarma (1988):

$$r = \frac{\sum_{i=1}^{n} \sin(x_i - \bar{x}) \sin(y_i - \bar{y})}{\sqrt{\sum_{i=1}^{n} \sin(x_i - \bar{x})^2} \sqrt{\sum_{i=1}^{n} \sin(y_i - \bar{y})^2}} \tag{3}$$

where x_i and y_i are aspect values (in radians) for pixel i, and $\bar{x}$ and $\bar{y}$ are circular means calculated as in Equation 2.

To calculate RMSEs for aspect, I did not attempt to use trigonometric properties analogous to computation of the circular correlation, but instead just imposed a simple correction whereby all pairwise differences were computed using the shorter of the two paths around the compass wheel

(Equation 4). For example, the difference between 0° and 150° is 150°, but the difference between 0° and 250° is 110°.

$$RMSE = \sqrt{\frac{\sum_{i=1}^{n}(\Delta_i^2)}{n}} \tag{4}$$
$$\text{where } \Delta_i = \text{argmin}\left(|x_i - y_i|, 360 - |x_i - y_i|\right)$$

Circular correlations between SRTM and ASTER were surprisingly low, typically hovering around 0.5, but dipping down towards zero at numerous latitudes (Figure 13a). The corresponding RMSE is close to 70 at all latitudes, surprisingly high considering that the maximum difference between any two pixels is 180° (Figure 13b). Comparison of SRTM and ASTER with CDED yields similar patterns.

For both of the blended layers (multiresolution spline and Gaussian weighted average), aspect values calculated in the zone of ASTER/SRTM overlap appear to be *less* similar to the component DEMs than those to data sources are to each other. As evident in the upper middle and upper right panels of Figure 13a, correlations between fused aspect and aspect based on the original SRTM and ASTER images are substantially *negative* for many latitudes in the zone of overlap. I don't have a good feel for what's going on here, although it may just involve properties of the circular correlation statistic that I don't have a good feel for. Note that the latitudinal profile of aspect RMSEs is less worrisome (upper middle and upper right panels of Figure 13b) and more closely resembles the profile of slope RMSEs discussed above, particularly as regards the more gradual transition in case of Gaussian weighted averaging compared to the multiresolution spline.

Flow direction As with aspect, circular correlation coefficients and adjusted RMSEs were calculated for each latitudinal band. Flow direction correlations between SRTM and ASTER are slightly lower than for aspect, typically around 0.40 but spiking negative at a handful of latitudes (Figure 13a). RMSEs hover consistently around ∼75, slightly lower than was the case with aspect (Figure 13b).

Aside from an expected flow artifact at the southern image edge, and an unexpected (and as-yet unexplained) negative spike at ∼59.95°N, the correlation profiles are fairly well-behaved for both blended layers, and don't show the same odd behavior as was the case for aspect. Again it is clear that the multiresolution spline results in a much more abrupt transition than does the Gaussian weighted average. The RMSE flow direction profiles echo this pattern (Figure 13b), and indeed look almost the same as those computed using aspect (Figure 12b).

Figure 1: Focal area used as the basis for boundary assessment. Note that for flow direction, analysis was restricted to a smaller longitudinal span (125°W to 100°W).

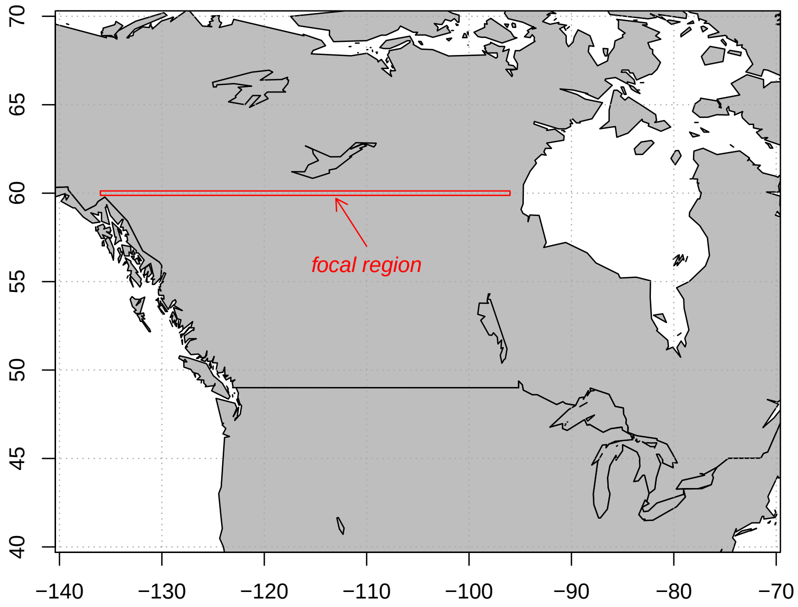

Figure 2: SRTM/ASTER DEM fusion configurations

(a) Simple fusion

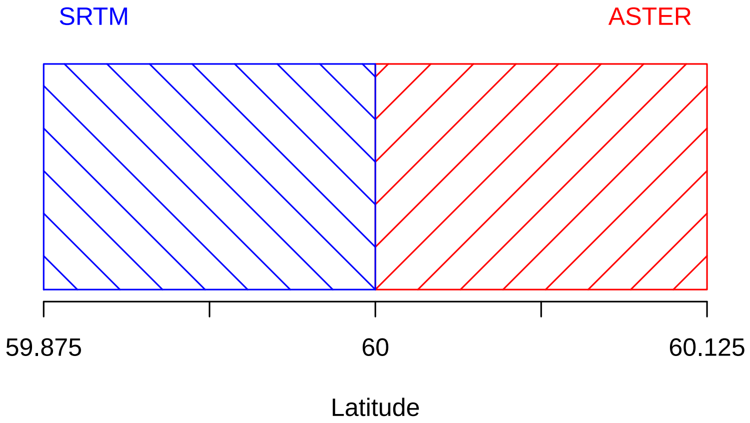

(b) Multiresolution spline

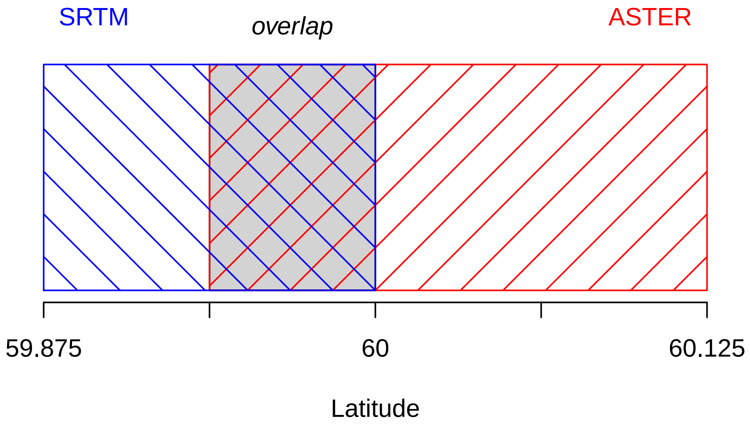

(c) Gaussian weighted average

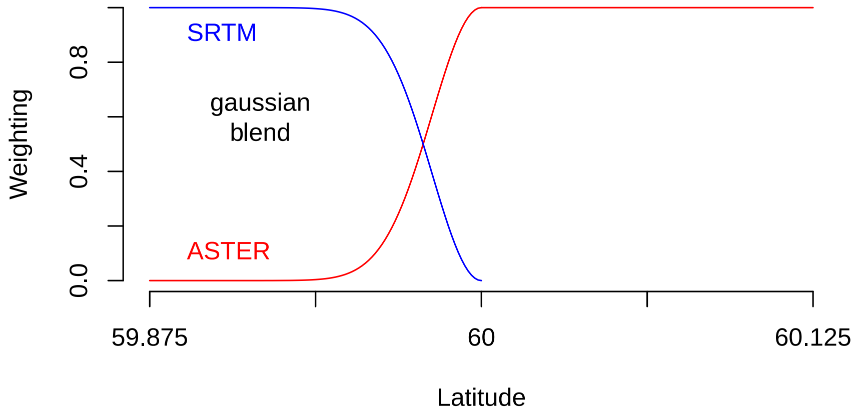

Figure 3: Mean elevation (m)

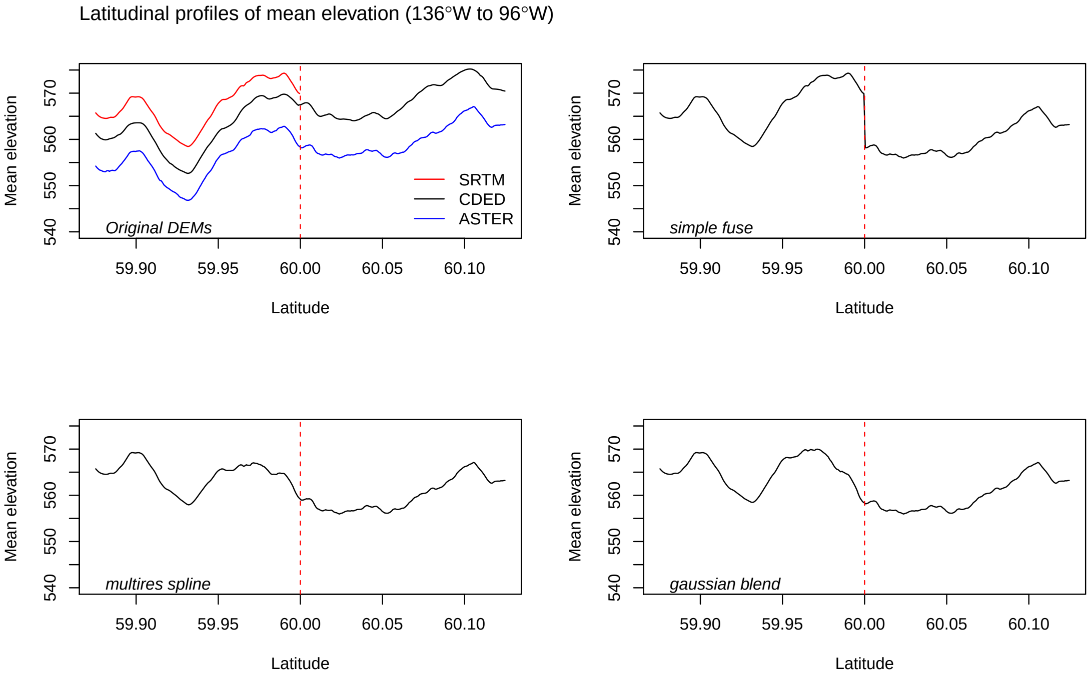
Latitudinal profiles of mean elevation (136°W to 96°W)

Figure 4: Mean slope (degrees)

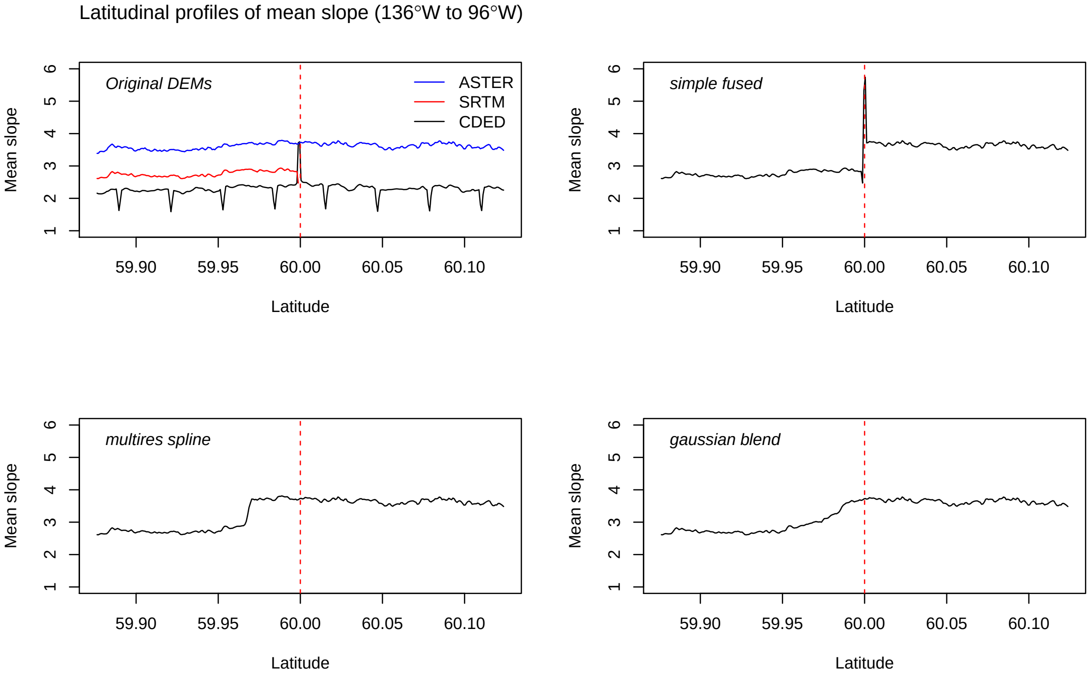
Latitudinal profiles of mean slope (136°W to 96°W)

Figure 5: Circular mean aspect (azimuth)

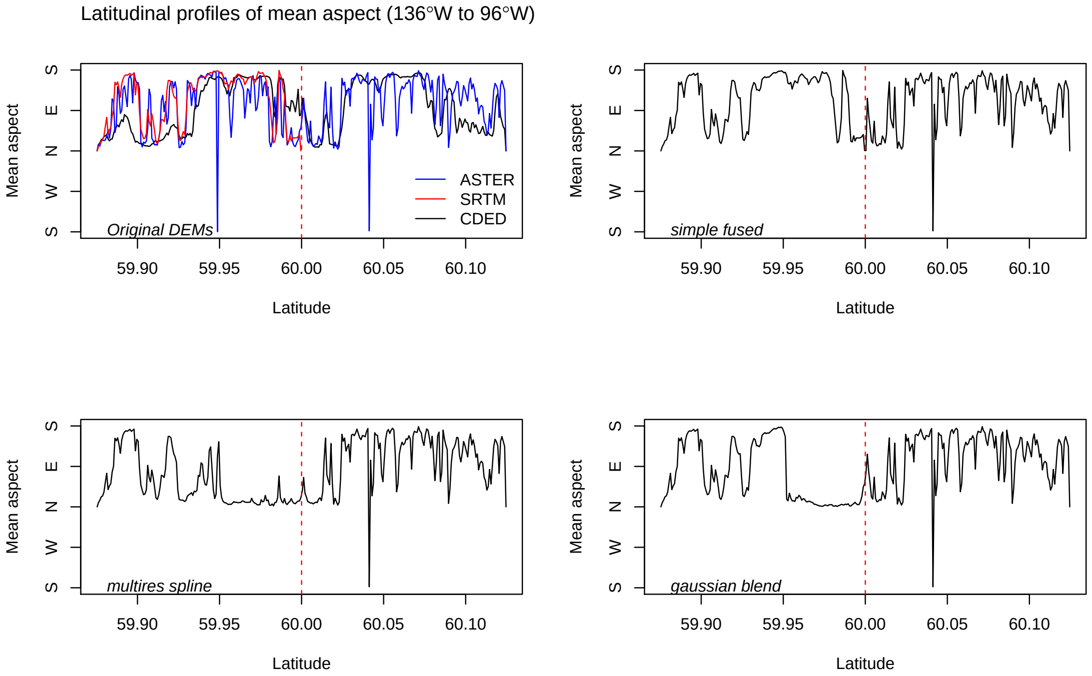

Figure 6: Circular mean flow direction

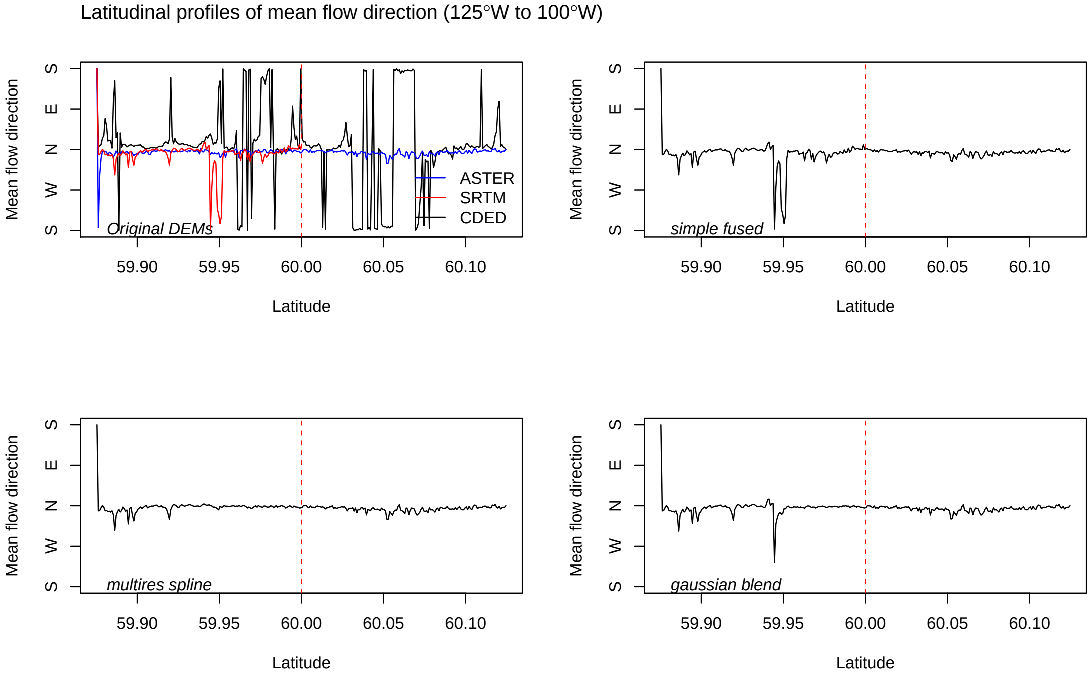

Figure 7: ASTER vs SRTM elevation comparisons

(a) Boxplots of the arithmetic difference in elevations (ASTER - SRTM), summarized across a series of SRTM elevation bins. Boxes include the median (horizontal band), 1st and 3rd quartiles (box extents), and ±1.5×IQR (whiskers); outliers not shown. Gray numbers above each whisker indicates how many thousands of pixels are included in the corresponding summary. Dashed red line indicates the median difference across all pixels south of 60°N.

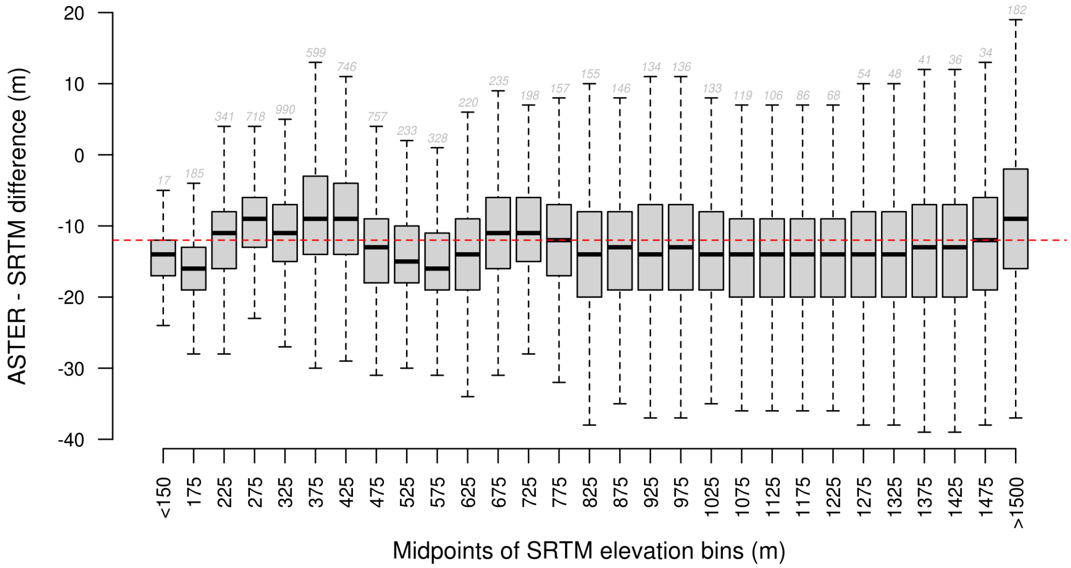

(b) Pixel-wise plot of SRTM vs ASTER for all values in the 150 latitudinal rows of overlap south of 60°N. Dashed blue line indicates the 1:1 diagonal, and the parallel red line is offset lower by the observed median difference between the two DEMs (12m). Inset histogram shows distribution of differences, excluding absolute differences >60m.

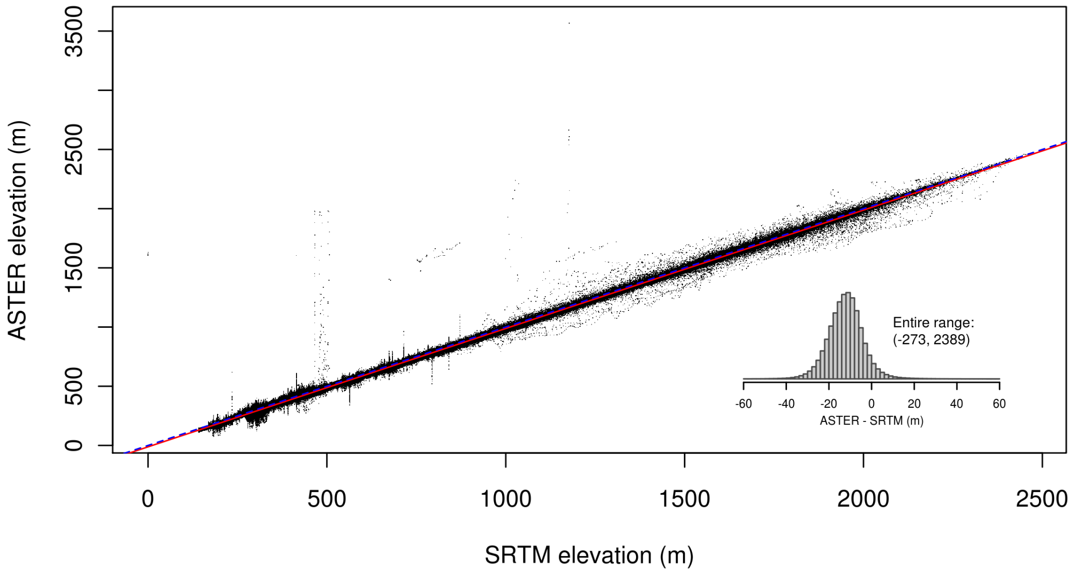

Figure 8: Binned frequency distributions of aspect within two selected latitudinal strips: (a) within the SRTM-ASTER blend zone, and (b) south of the overlap zone. Aspect values here are based on the DEM produced via Gaussian weighted averaging, but similar patterns are evident using the other DEMs. Red spoke lines indicate the circular mean direction across all pixels at the associated latitude.

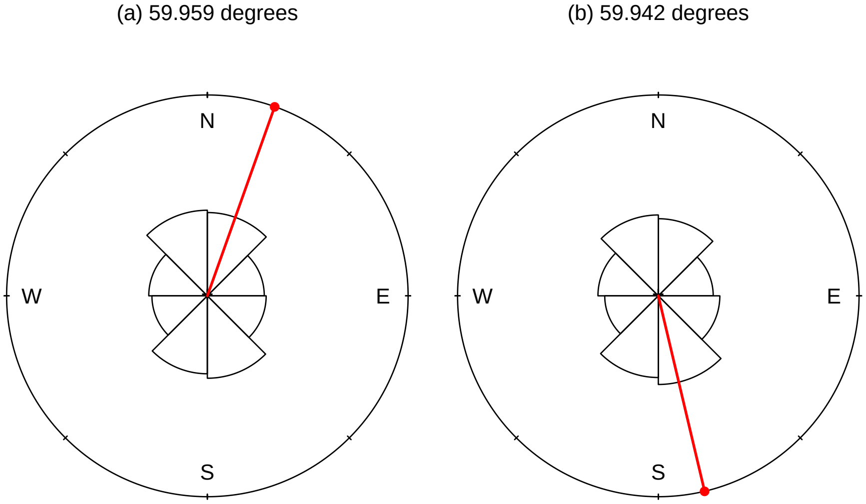

Figure 9: Relative frequencies of D8 flow directions (indicated by relative heights of the blue spokes) within two selected latitudinal bands: (a) within the SRTM-ASTER blend zone, and (b) south of the overlap zone. Flow directions here are based on the DEM produced via Gaussian weighted averaging. Red spoke lines indicate the circular mean flow direction across all pixels at the associated latitude.

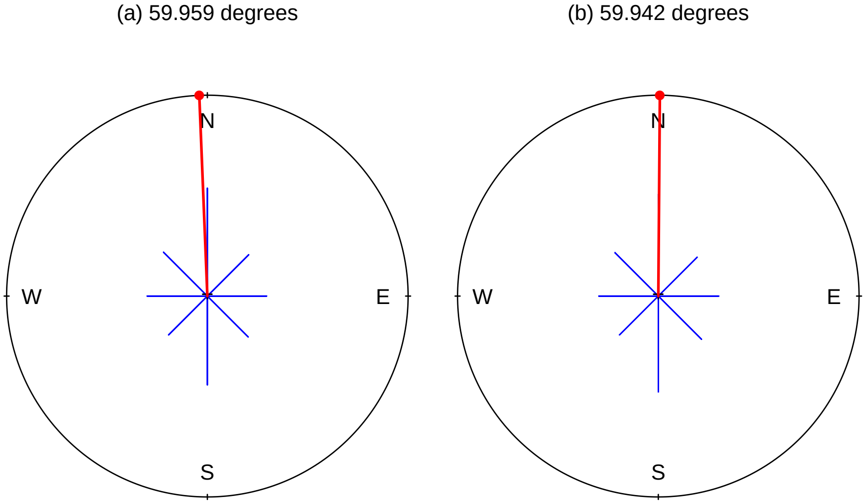

Figure 10: Elevation associations between original and fused layers

(a) Elevation correlations

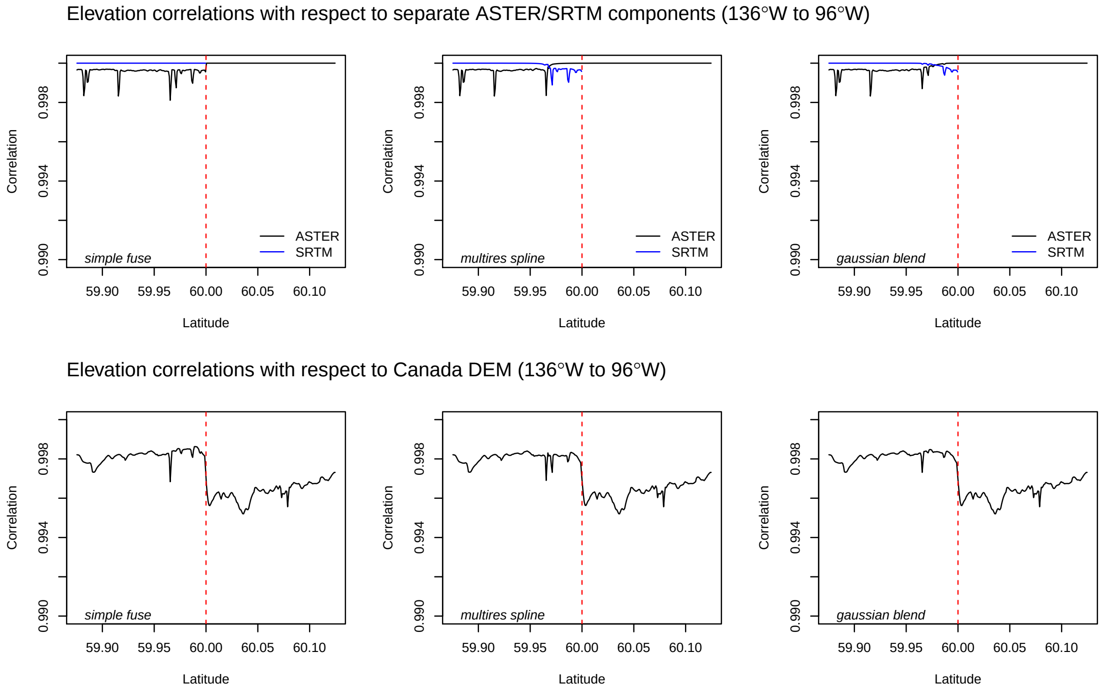

(b) Elevation RMSEs

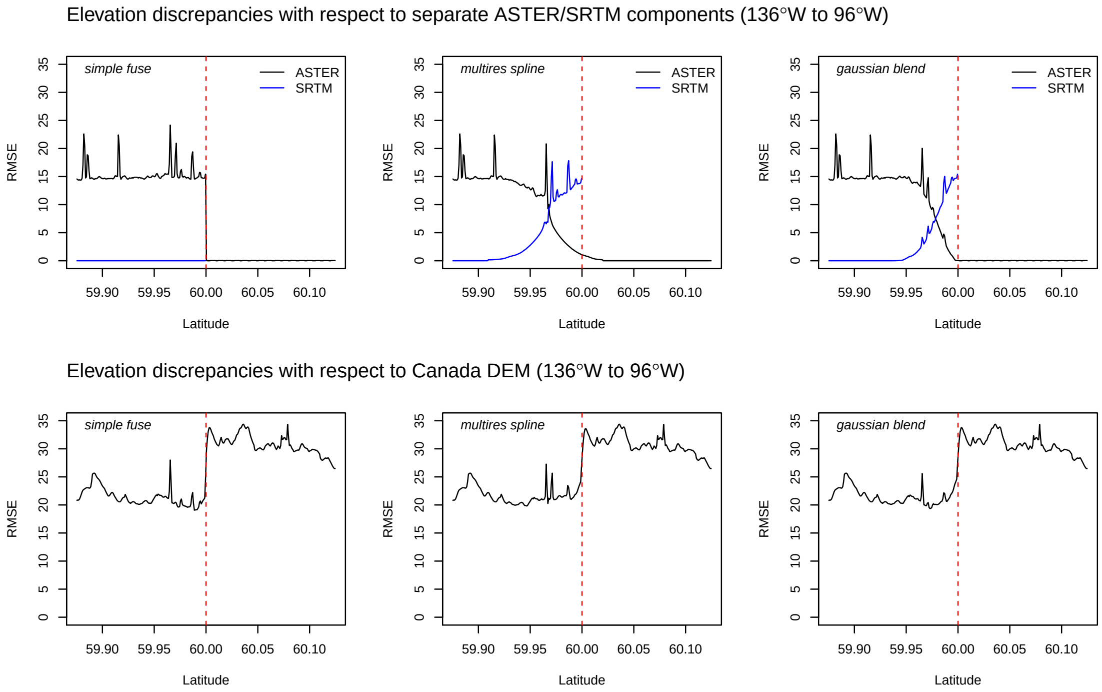

Figure 11: Slope associations between original and fused layers

(a) Slope correlations

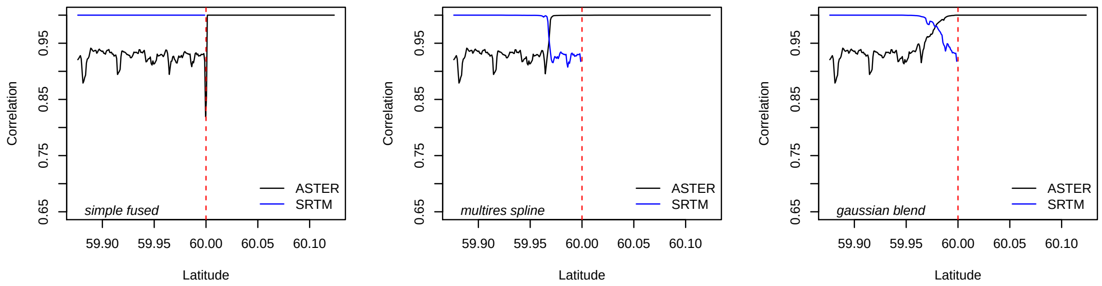
Slope correlations with respect to separate ASTER/SRTM components (136°W to 96°W)

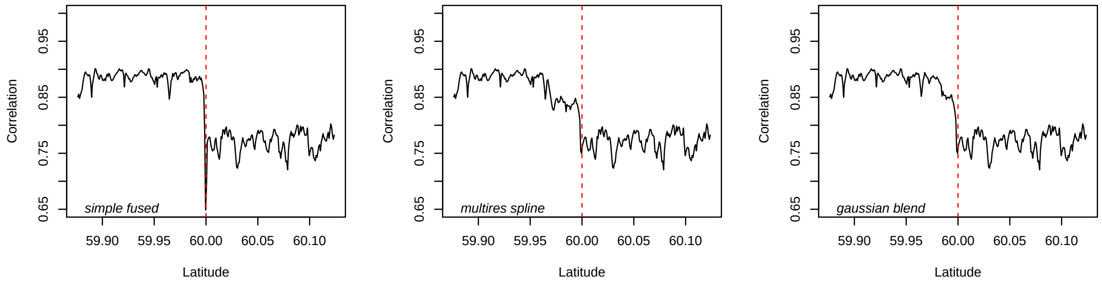
Slope correlations with respect to Canada DEM (136°W to 96°W)

(b) Slope RMSEs

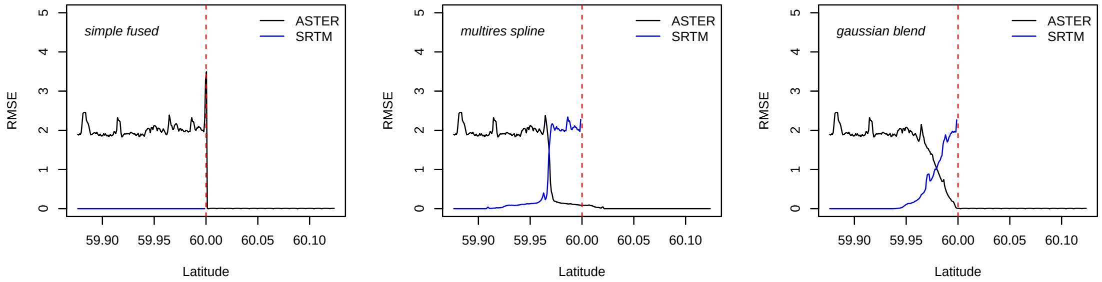
Slope discrepancies with respect to separate ASTER/SRTM components (136°W to 96°W)

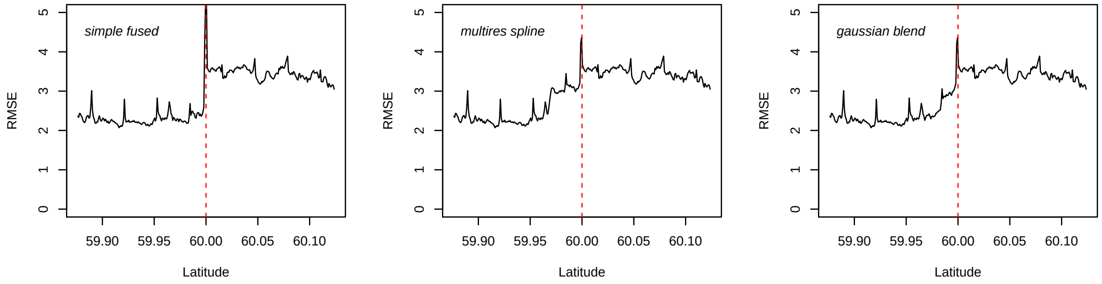
Slope discrepancies with respect to Canada DEM (136°W to 96°W)

Figure 12: Aspect associations between original and fused layers

(a) Aspect circular correlations

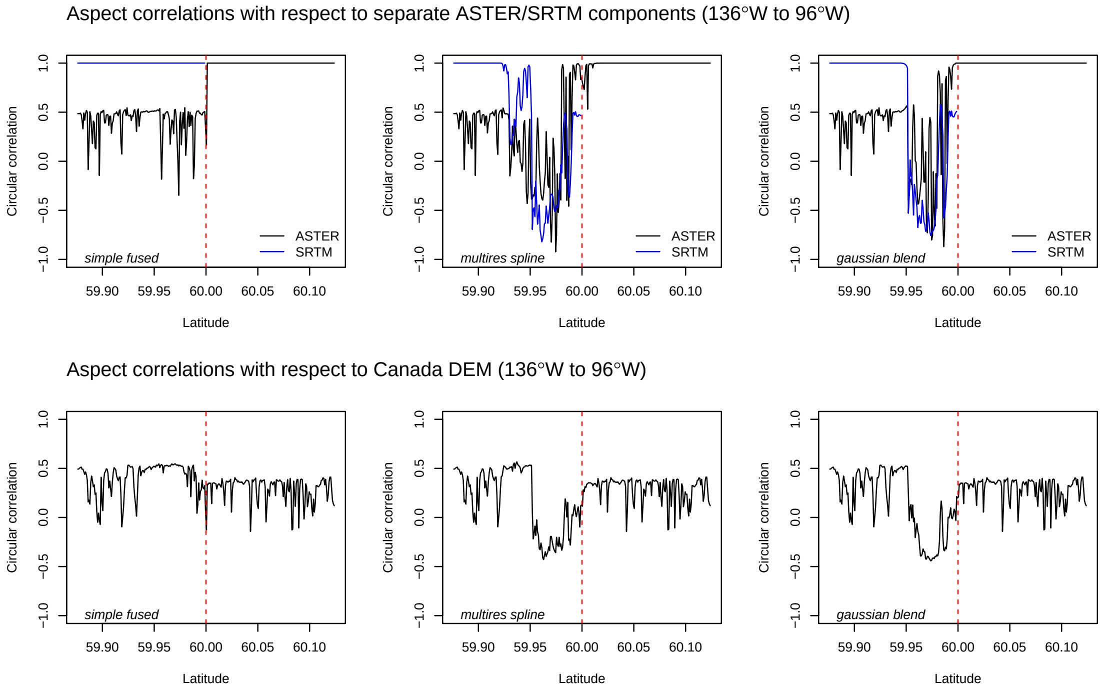

(b) Aspect RMSEs

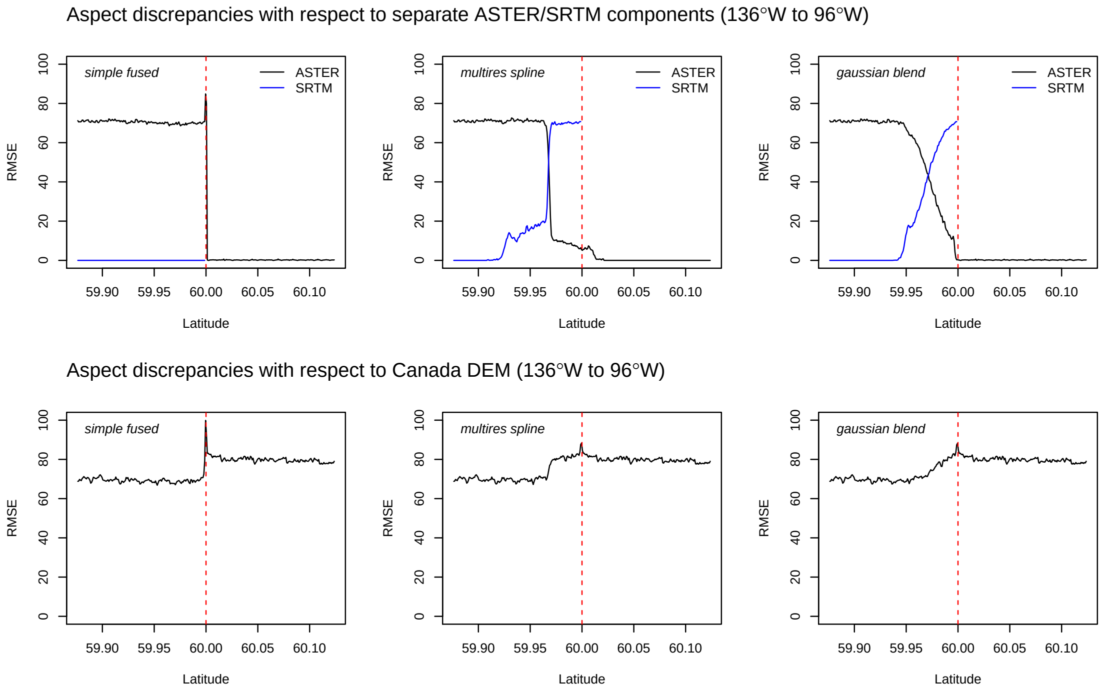

Figure 13: Flow direction associations between original and fused layers

(a) Flow direction correlations

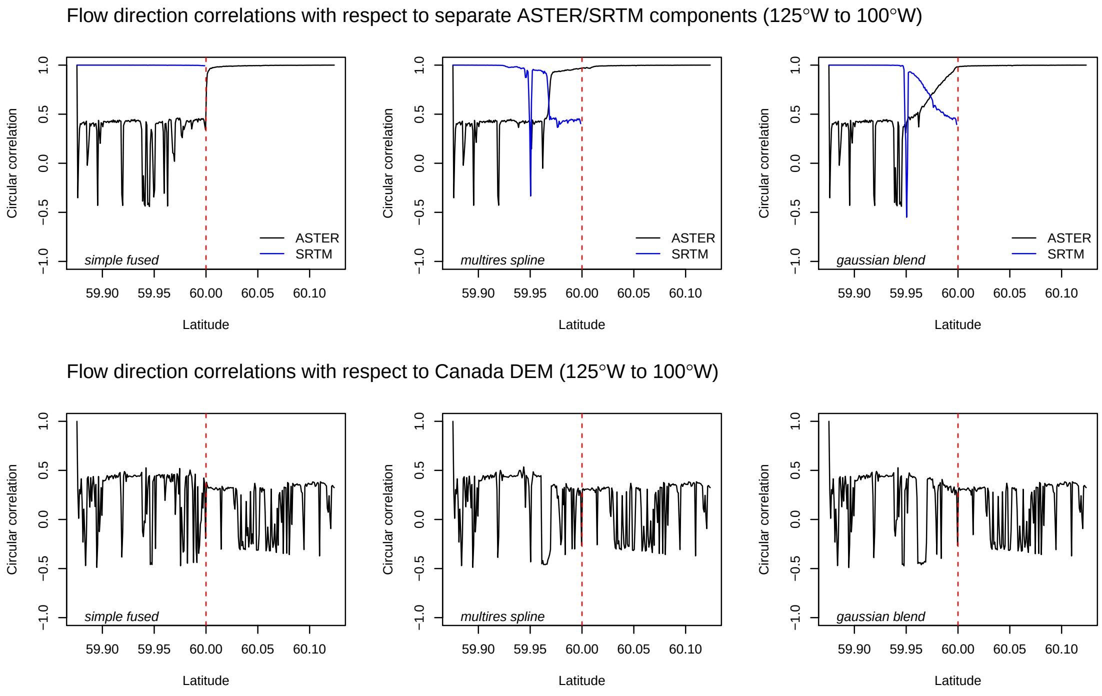

(b) Flow direction RMSEs

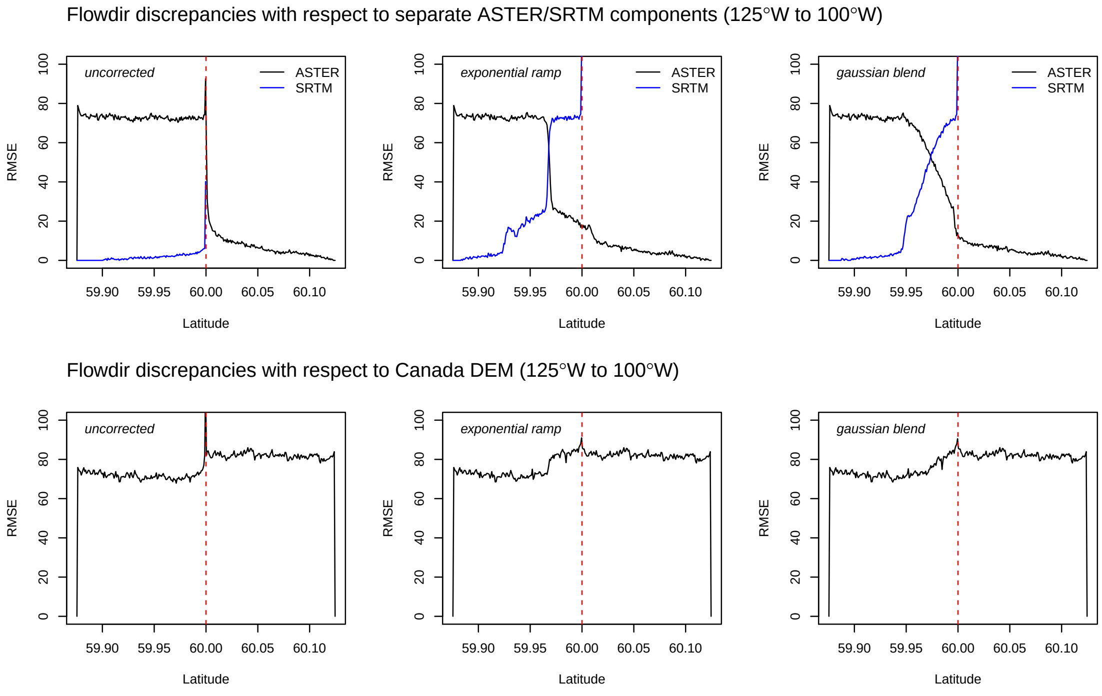

Code listings

Listing 1: GDAL commands for assembling and resampling SRTM and ASTER tiles into GeoTIFFs for use as inputs to the boundary correction routines described in this document.

```
# GDAL commands for assembling SRTM and ASTER DEM tiles associated with
# the 60N Canada boundary analysis, and resampling into the desired 3"
# (~90m) resolution even-boundary grid.
#
# These commands generate strips of elevation data (GeoTIFFs) along a
# 40-degree longitudinal extent matching (at least one of) Rick Reeves'
# mosaicked CDEM grids. The strips extend 150 pixels south of 60N and
# (in case of ASTER only) 150 pixels north of 60N, which should provide
# a sufficient but not excessive latitudinal range for fixing and
# assessing boundary artifacts.
#
# Note:
#   Working with the original ASTERs yields this warning from GDAL:
#     Warning 1: TIFFReadDirectoryCheckOrder:Invalid TIFF directory;
#     tags are not sorted in ascending order
#   I then ran gdal_translate on several of the offending ASTERs, then
#   repeated the vrt/warp on those -- now without warnings. However, the
#   output data was the same as when I operated on the original files
#   (with warnings), so for the moment I'm just going to ignore the
#   warnings.
#
# Jim Regetz
# NCEAS

# at the time of script creation, these paths were correct on vulcan
export ASTDIR="/home/reeves/active_work/EandO/asterGdem"
export SRTMDIR="/home/reeves/active_work/EandO/CgiarSrtm/SRTM_90m_ASCII_4_1"

# SRTM (also convert to 16bit integer)
gdalbuildvrt srtm.vrt $SRTMDIR/srtm_*_01.asc
gdalwarp -ot Int16 -te -136 59.875 -96 60 -ts 48000 150 -r bilinear \
  srtm.vrt srtm_150below.tif

# ASTER
gdalbuildvrt aster.vrt $ASTDIR/ASTGTM_N59*W*_dem.tif \
  $ASTDIR/ASTGTM_N60*W*_dem.tif
gdalwarp -te -136 59.875 -96 60 -ts 48000 150 -r bilinear \
  aster.vrt aster_150below.tif
gdalwarp -te -136 60 -96 60.125 -ts 48000 150 -r bilinear \
  aster.vrt aster_150above.tif

# note that the top 150 rows of this one are, somewhat surprisingly,
# slightly different from the above!
# gdalwarp -te -136 59.875 -96 60.125 -ts 48000 300 -r bilinear \
#   aster.vrt aster_300straddle.tif
#
# and this yields an even different set of values
# gdalbuildvrt aster_N60.vrt £ASTDIR/ASTGTM_N60*W*_dem.tif
# gdalwarp -te -136 60 -96 60.125 -ts 48000 150 -r bilinear \
#   aster_N60.vrt aster_150above.tif
```

Listing 2: R code implementing several SRTM-ASTER boundary corrections, including the Gaussian weighted average layer discussed in this document (see `OPTION 3`, as identified in code comments).

```
# R script to apply several kinds of boundary corrections to ASTER/SRTM
# elevation values near the 60N boundary in Canada, and write out new
# GeoTIFFs.
#
# Jim Regetz
# NCEAS

library(raster)

# load relevant SRTM and ASTER data
srtm.south <- raster("srtm_150below.tif")
aster.south <- raster("aster_150below.tif")
aster.north <- raster("aster_150above.tif")

# create difference raster for area of overlap
delta.south <- srtm.south - aster.south


#
# OPTION 1
#

# smooth to the north, by calculating the deltas _at_ the boundary,
# ramping them down to zero with increasing distance from the border,
# and adding them to the north ASTER values

# create simple grid indicating distance (in units of pixels) north from
# boundary, starting at 1 (this is used for both option 1 and option 2)
aster.north.matrix <- as.matrix(aster.north)
ydistN <- nrow(aster.north.matrix) + 1 - row(aster.north.matrix)

# 1a. linear ramp north from SRTM edge
# -- Rick has done this --

# 1b. exponential ramp north from SRTM edge
r <- -0.045
w <- exp(ydistN*r)
aster.north.smooth <- aster.north
aster.north.smooth[] <- values(aster.north) + as.integer(round(t(w) *
    as.matrix(delta.south)[1,]))
writeRaster(aster.north.smooth, file="aster_150above_rampexp.tif")

#
# OPTION 2
#

# smooth to the north, by first using LOESS with values south of 60N to
# model deltas as a function of observed ASTER, then applying the model
# to predict pixel-wise deltas north of 60N, then ramping these
# predicted deltas to zero with increasing distance from the border, and
# adding them to the associated ASTER values

# first fit LOESS on a random subsample of data
# note: doing all the data takes too long, and even doing 50k points
#       seems to be too much for calculating SEs during predict step
set.seed(99)
samp <- sample(ncell(aster.south), 10000)
sampdata <- data.frame(delta=values(delta.south)[samp],
    aster=values(aster.south)[samp])
lo.byaster <- loess(delta ~ aster, data=sampdata)

# now create ASTER prediction grid north of 60N
# TODO: deal with NAs in data (or make sure they are passed through
#       properly in the absence of explicit treatment)?
aster.north.pdelta <- aster.north
aster.north.pdelta[] <- predict(lo.byaster, values(aster.north))
```

```
# for actual north ASTER values that exceed the max value used to fit
# LOESS, just use the prediction associated with the maximum
aster.north.pdelta[aster.north<min(sampdata$aster)] <- predict(lo.byaster,
    data.frame(aster=min(sampdata$aster)))
# for actual north ASTER value less than the min value used to fit
# LOESS, just use the prediction associated with the minimum
aster.north.pdelta[aster.north>max(sampdata$aster)] <- predict(lo.byaster,
    data.frame(aster=max(sampdata$aster)))

# 2a: exponential distance-weighting of LOESS predicted deltas
r <- -0.045
w <- exp(r*ydistN)
aster.north.smooth <- aster.north
aster.north.smooth[] <- values(aster.north) + as.integer(round(t(w *
    as.matrix(aster.north.pdelta))))
writeRaster(aster.north.smooth, file="aster_150above_predexp.tif")

# 2b: gaussian distance-weighting of LOESS predicted deltas
r <- -0.001  # weight drops to 0.5 at ~26 cells, ie 2.4km at 3" res
w <- exp(r*ydistN^2)
aster.north.smooth <- aster.north
aster.north.smooth[] <- values(aster.north) + as.integer(round(t(w *
    as.matrix(aster.north.pdelta))))
writeRaster(aster.north.smooth, file="aster_150above_predgau.tif")

#
# OPTION 3
#

# smooth to the south, now by simply taking pixel-wise averages of the
# observed SRTM and ASTER using a distance-based weighting function such
# that the relative contribution of ASTER decays to zero over a few km

# create simple grid indicating distance (in units of pixels) south from
# boundary, starting at 1
aster.south.matrix <- as.matrix(aster.south)
ydistS <- row(aster.south.matrix)

# 3a: gaussian weighting function
r <- -0.001  # weight drops to 0.5 at ~26 cells, or 2.4km at 3" res
w <- exp(-0.001*ydistS^2)
aster.south.smooth <- aster.south
aster.south.smooth[] <- values(srtm.south) - as.integer(round(t(w *
    as.matrix(delta.south))))
aster.south.smooth[aster.south.smooth<0] <- 0
writeRaster(aster.south.smooth, file="dem_150below_blendgau.tif")
```

Listing 3: GDAL commands for assembling boundary-corrected DEM components above and below 60°N, for each of several correction approaches implemented in Listing 2. Note that multiresolution spline blending is treated separately (see Listing 4).

```
# GDAL commands to produced fused DEMs in the vicinity of the 60N Canada
# boundary, using several "boundary-corrected" variants as well as the
# original uncorrected DEMs. Note that the multiresolution spline is not
# included here, because the associated fused layer is already produced
# in its entirety during that process.
#
# Jim Regetz
# NCEAS

# uncorrected fused layer
gdalwarp -ot Int16 -te -136 59.875 -96 60.125 -ts 48000 300 \
  srtm_150below.tif aster_150above.tif fused_300straddle.tif

# exponential ramp of boundary delta to the north
gdalwarp -ot Int16 -te -136 59.875 -96 60.125 -ts 48000 300 \
  srtm_150below.tif aster_150above_rampexp.tif fused_300straddle_rampexp.tif

# exponential blend of predicted deltas to the north
gdalwarp -ot Int16 -te -136 59.875 -96 60.125 -ts 48000 300 \
  srtm_150below.tif aster_150above_predexp.tif fused_300straddle_predexp.tif

# gaussian blend of predicted deltas to the north
gdalwarp -ot Int16 -te -136 59.875 -96 60.125 -ts 48000 300 \
  srtm_150below.tif aster_150above_predgau.tif fused_300straddle_predgau.tif

# gaussian blend of SRTM/ASTER to the south
gdalwarp -ot Int16 -te -136 59.875 -96 60.125 -ts 48000 300 \
  dem_150below_blendgau.tif aster_150above.tif fused_300straddle_blendgau.tif
```

Listing 4: R wrapper code for multiresolution spline of SRTM and ASTER.

```
# Code to produce enblended DEM (i.e., using multiresolution splines as
# described by Burt & Adelson 1983) in the 60N boundary region. After
# appropriately preparing the SRTM and ASTER layers, this code makes a
# system call to run 'enblend' (v. 4.0) on the inputs, then
# post-processes the resulting image to yield a single band geotiff with
# datatype of 16bit signed integer, matching the input data.
#
# Somewhat arbitrarily, in the code below the input DEMs are prepped
# such that the area of SRTM/ASTER overlap is the first 75 rows below
# 60N (i.e., a zone extending ~6.75km south of the boundary).
#
# Jim Regetz
# NCEAS

library(raster)

demdir <- "/home/regetz/media/temp/terrain/dem"

# read in aster data
aster <- raster(file.path(demdir, "aster_300straddle.tif"))
# create alpha layer for aster
alpha <- aster
alpha[] <- 0
alpha[1:225, ] <- 1
# write enblend-ready tif out to disk
writeRaster(brick(aster, alpha), file="aster-enblend.tif",
    options="ALPHA=YES")

# read in srtm
srtm.lower <- raster("../srtm_150below.tif")
# expand to match full image (i.e., same extent as aster), holding srtm
# data below 60N and nothing above
srtm <- aster
srtm[] <- NA
srtm[151:300, ] <- values(srtm.lower)
# create alpha layer for srtm
alpha <- srtm
alpha[] <- 0
alpha[151:300, ] <- 1
writeRaster(brick(srtm, alpha), file="srtm-enblend.tif",
    options="ALPHA=YES")

# run 'enblend'
system(paste("enblend --verbose=6 -o enblend.tif",
    "aster-enblend.tif srtm-enblend.tif"))

# post-process enblended DEM
e <- raster("enblend.tif")
e2 <- aster
# round to nearest integer, and write out the result as a geotiff
e2[] <- as.integer(round(values(e), 0))
writeRaster(e2, file=file.path(demdir, "fused_300straddle_enblend.tif"),
    options="COMPRESS=NONE", datatype="INT2S")
```

Listing 5: GRASS code for computing flow directions using the various fused elevation rasters and their components DEMS as inputs.

```
# GRASS commands for running terraflow on raw and fused DEMs in the
# 60N Canada boundary region, currently for the purposes of assessing
# and comparing flow direction.
#
# Jim Regetz
# NCEAS

export DEMDIR=~/media/temp/terrain/dem
export FLOWDIR=~/media/temp/terrain/flow

#
# Canada near 60N, from 136W to 96WW
#

# load sample data for testing flow stuff
r.in.gdal input=$DEMDIR/cdem_300straddle.tif output=cdem_300straddle
r.in.gdal input=$DEMDIR/aster_300straddle.tif output=aster_300straddle
r.in.gdal input=$DEMDIR/srtm_150below.tif output=srtm_150below
r.in.gdal input=$DEMDIR/fused_300straddle.tif output=fused_300straddle
r.in.gdal input=$DEMDIR/fused_300straddle_rampexp.tif output=fused_300straddle_rampexp
r.in.gdal input=$DEMDIR/fused_300straddle_blendgau.tif output=fused_300straddle_blendgau
r.in.gdal input=$DEMDIR/fused_300straddle_enblend.tif output=fused_300straddle_enblend

# oops -- region is too big for terraflow default of using
# dimension_type (i.e., short), which means nrows and ncols are both
# capped at ~30K (2^15):
#  ERROR: [nrows=300, ncols=48000] dimension_type overflow -- change
#         dimension_type and recompile
# so let's restrict it to a smaller lon range for now...
g.region n=60.125 s=59.875 w=-125 e=-100

# do flow
# each took ~1.5 min on xander (22-Jun-2011)
r.terraflow.short elevation=cdem_300straddle filled=filled_cdem \
  direction=direction_cdem swatershed=swatershed_cdem \
  accumulation=accumulation_cdem tci=tci_cdem
r.terraflow.short elevation=aster_300straddle filled=filled_aster \
  direction=direction_aster swatershed=swatershed_aster \
  accumulation=accumulation_aster tci=tci_aster
r.terraflow.short elevation=fused_300straddle filled=filled_fused \
  direction=direction_fused swatershed=swatershed_fused \
  accumulation=accumulation_fused tci=tci_fused
r.terraflow.short elevation=fused_300straddle_blendgau filled=filled_fused_bg \
  direction=direction_fused_bg swatershed=swatershed_fused_bg \
  accumulation=accumulation_fused_bg tci=tci_fused_bg
r.terraflow.short elevation=fused_300straddle_enblend filled=filled_fused_mrs \
  direction=direction_fused_mrs swatershed=swatershed_fused_mrs \
  accumulation=accumulation_fused_mrs tci=tci_fused_mrs

# now with SFD (D8) algorithm
# each took ~1 min on xander (22-Jun-2011)
r.terraflow.short -s elevation=cdem_300straddle filled=filled_cdem_sfd \
  direction=direction_cdem_sfd swatershed=swatershed_cdem_sfd \
  accumulation=accumulation_cdem_sfd tci=tci_cdem_sfd
r.terraflow.short -s elevation=aster_300straddle filled=filled_aster_sfd \
  direction=direction_aster_sfd swatershed=swatershed_aster_sfd \
  accumulation=accumulation_aster_sfd tci=tci_aster_sfd
r.terraflow.short -s elevation=fused_300straddle filled=filled_fused_sfd \
  direction=direction_fused_sfd swatershed=swatershed_fused_sfd \
  accumulation=accumulation_fused_sfd tci=tci_fused_sfd
r.terraflow.short -s elevation=fused_300straddle_blendgau filled=filled_fused_bg_sfd \
  direction=direction_fused_bg_sfd swatershed=swatershed_fused_bg_sfd \
  accumulation=accumulation_fused_bg_sfd tci=tci_fused_bg_sfd
r.terraflow.short -s elevation=fused_300straddle_enblend filled=filled_fused_mrs_sfd \
  direction=direction_fused_mrs_sfd swatershed=swatershed_fused_mrs_sfd \
```

```
  accumulation=accumulation_fused_mrs_sfd tci=tci_fused_mrs_sfd

# export flow dir rasters as geotiffs
r.out.gdal input=direction_cdem output=$FLOWDIR/cdem_300straddle_mfd.tif
r.out.gdal input=direction_cdem_sfd output=$FLOWDIR/cdem_300straddle_sfd.tif
r.out.gdal input=direction_aster output=$FLOWDIR/aster_300straddle_mfd.tif
r.out.gdal input=direction_aster_sfd output=$FLOWDIR/aster_300straddle_sfd.tif
r.out.gdal input=direction_fused output=$FLOWDIR/fused_300straddle_mfd.tif
r.out.gdal input=direction_fused_sfd output=$FLOWDIR/fused_300straddle_sfd.tif
r.out.gdal input=direction_fused_bg output=$FLOWDIR/fused_300straddle_blendgau_mfd.tif
r.out.gdal input=direction_fused_bg_sfd output=$FLOWDIR/fused_300straddle_blendgau_sfd.tif
r.out.gdal input=direction_fused_mrs output=$FLOWDIR/fused_300straddle_enblend_mfd.tif
r.out.gdal input=direction_fused_mrs_sfd output=$FLOWDIR/fused_300straddle_enblend_sfd.tif

# export flow accumulation
r.out.gdal input=accumulation_fused_bg output=$FLOWDIR/fused_300straddle_blendgau_fa.tif
r.out.gdal input=accumulation_cdem output=$FLOWDIR/cdem_300straddle_fa.tif
r.out.gdal input=accumulation_aster output=$FLOWDIR/aster_300straddle_fa.tif

# do the above for SRTM, but only in southern half of region
g.region n=60 s=59.875 w=-125 e=-100
r.terraflow.short elevation=srtm_150below filled=filled_srtm \
  direction=direction_srtm swatershed=swatershed_srtm \
  accumulation=accumulation_srtm tci=tci_srtm
r.terraflow.short -s elevation=srtm_150below filled=filled_srtm_sfd \
  direction=direction_srtm_sfd swatershed=swatershed_srtm_sfd \
  accumulation=accumulation_srtm_sfd tci=tci_srtm_sfd
r.out.gdal input=direction_srtm output=$FLOWDIR/srtm_150below_mfd.tif
r.out.gdal input=direction_srtm_sfd output=$FLOWDIR/srtm_150below_sfd.tif
r.out.gdal input=accumulation_srtm output=$FLOWDIR/srtm_150below_fa.tif
# don't forget to set the region back to include cells above the 60N boundary...
g.region n=60.125 s=59.875 w=-125 e=-100
```